Analysis of High-Aspect Ratio Jet-Flap Wings of Arbitrary Geometry

P. B. S. Lissaman*
AeroVironment Inc., Pasadena, Calif.

This paper presents a design technique for rapidly computing lift, induced drag, and spanwise loading of unswept, uncambered jet-flap wings of arbitrary thickness, chord, twist, blowing, and jet angle, including discontinuities. Linear theory is used, extending Spence's method for elliptically loaded jet-flap wings. Curves for uniformly blown rectangular wings are presented for direct performance estimation. Arbitrary planforms require a simple computer program. Results correlate with limited existing data, and show lifting line theory is reasonable down to an aspect ratio of 5.

Introduction

POWERED lift is becoming an increasingly important technique for STOL vehicles. In general, this consists of methods in which the energy of a certain mass of air is increased, and this mass then forced over aerodynamic surfaces to amplify the lifting effects. Typical examples of powered lift using a jet sheet with lifting-surface interaction are: jet-flap wing, externally blown flap, and augmentor wing. The theory developed in this analysis is applicable to all these types of lift amplification, since augmentor wings and externally blown flaps involve a similar analysis to jet-flap wings and may be approximated by thin jet-flap theory.

For the problem considered, a high-energy jet sheet issuing from the trailing edge of the wing is assumed. The standard assumptions of incompressible inviscid flow, a thin jet, and linearized boundary conditions are made. This model is described in detail in Ref. 1.

The linearized problem for the two-dimensional jet flap both in and out of ground effect has been treated in Ref. 2 and 3. Excellent correlation of the theory with experiment has been found. The three-dimensional problem has been handled by a number of workers using different approaches to handle the kinematic and dynamic boundary conditions in the wake.[4-8] The model by Maskell and Spence[1] handles the dynamic condition on the wake by using two-dimensional solutions which approximately match the boundary conditions. However, this treats only the high-aspect-ratio elliptically loaded case. The most comprehensive model is that given by Lopez and Shen.[8] Although this model (like the others) is linearized, it utilizes lifting-surface theory, finding the wake deformation by interaction on the proper dynamic and kinematic boundary conditions.

The model proposed here lies somewhere between that of Ref. 1 and Ref. 8 in its assumptions and complexity. It is an extension of the blown lifting-line concept for a high-aspect-ratio wing of arbitrary planform and blowing taking into account discontinuities in the wing geometry in chord, angle of attack, jet angle, or blowing coefficient.

Presented as Paper 73-125 at the AIAA 11th Aerospace Sciences Meeting, Washington, D.C., January 10-12, 1973; submitted January 29, 1973; revision received January 14, 1974. This research was sponsored by the NASA Langley Research Center under Contract NAS1-10627. The major portion of the work was done while the author was at Northrop Corporate Laboratories, Hawthorne, Calif.

Index categories: Aircraft Aerodynamics (Including Component Aerodynamics); Aircraft Performance; Subsonic and Transonic Flow.

*Director, Aerosciences. Associate Fellow AIAA.

Analysis

General

The basic idea, which may be formalized in terms of matched asymptotic expansions, is that the forces on the wing may be determined in two places. In the Trefftz plane, the forces may be uniquely determined in terms of wake parameters (downwash and jet coefficient). On the wing itself (wing plane), the forces may be determined in terms of local section properties. Here, the main parameters are the blown airfoil characteristics and the induced downwash angle at the wing. The Trefftz plane and wing plane forces are then matched to provide sufficient equations for solution.

In the case of an unblown wing, the lift in the two planes is matched to provide a relationship between the potential ϕ and the Trefftz plane downwash ϕ_y, generating the well-known integrodifferential equation of lifting theory (Prandtl's equation). An important assumption is that the induced angle at the wing is taken to be half that in the Trefftz plane. For a blown wing, a major portion of the bound vorticity (that directly due to the jet sheet) is located downstream of the trailing edge. It is not correct to assume that all the trailing vorticity emanates from a lifting line situated within the wing chord, so the above induced angle assumption is invalid. The analysis involves only two space variables, with the coordinate system centered on the wing or wake centerline (Fig. 1).

The approach of Ref. 1 is adopted, and introduces a new constant σ (variable across the span) by which the Trefftz plane downwash is scaled. Thus, the downwash at the wing is assumed constant at each chordwise station and equal to $\sigma(x)\alpha_\infty(x)$ where α (x) is the downwash angle

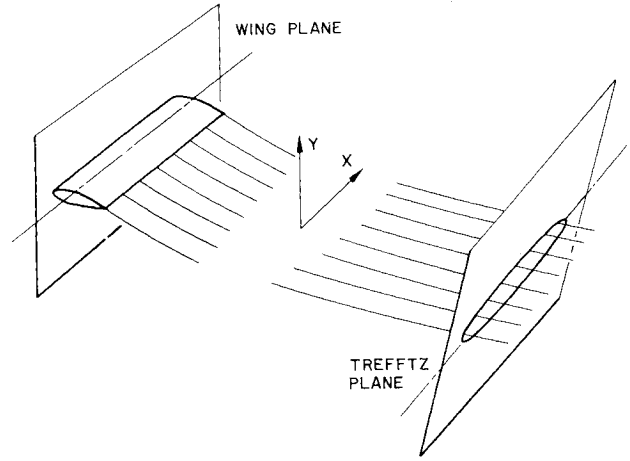

Fig. 1 Geometry of spanwise planes.

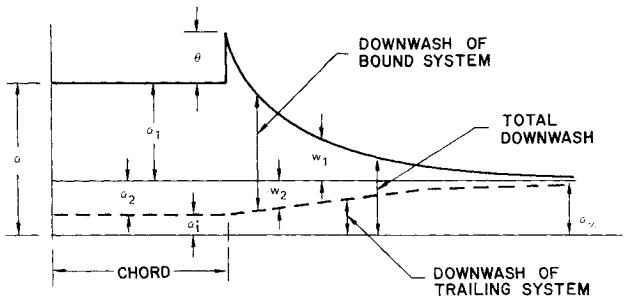

Fig. 2 Chordwise downwash of jet flap wing.

in the Trefftz plane. Hence, the induced angle $\alpha_i(x)$ (Fig. 2) is given by

$$\alpha_i(x) = \sigma(x)\alpha_\infty(x) \tag{1}$$

Thus a further unknown is introduced into the wing plane solution, so that an additional matching equation is required. It seems natural then to match both the lift and drag equations, or equivalently, the normal and chordwise force equations providing the additional equation for σ. Reference 1 assumes that σ is constant across the span, as implied by the elliptical loading. In the present solution, σ is permitted to vary with x and determined at each spanwise station.

Note that, in this paper, σ is defined as the ratio of the induced angle at the wing to that at infinity. In Ref. 1 a different definition for σ is used. Thus our σ is not the same as that of Ref. 1; for example, for an unblown wing the present paper gives $\sigma = \frac{1}{2}$ while Ref. 1 would give $\sigma = 0$.

Trefftz Plane Solution

By considering the flow in the Trefftz plane and by resolving parallel and normal to the chord, a pair of equations is obtained for the normal pressure coefficient and the thrust coefficient on the wing. The total force on the wing constitutes the sum of the pressure force and the momentum force due to the jet. Since the latter can be directly computed from the kinematics, it is more convenient to work with the pressure forces alone. All coefficients are normalized by division of the dimensional force by $\frac{1}{2}\rho V^2 c$ for the two-dimensional quantities and by $\frac{1}{2}\rho V^2 S_W$ for the integrated wing quantities, where ρ is the ambient density, V the freestream velocity, c the local chord, and S_W the wing area. Reference 9 shows these force coefficients to be given by

$$C_n = 4\bar{\alpha}\,\phi/c - C_j(\bar{\alpha}\phi_y + \alpha + \theta) \tag{2}$$

$$2C_t = (4\bar{\alpha}\phi/c)(\alpha + \bar{\alpha}\phi_y) + C_j\{\theta^2 - (\alpha + \bar{\alpha}\phi_y)^2\} \tag{3}$$

Here θ is the jet angle, $\bar{\alpha}\phi$ is the potential normalized by V.

Wing Plane Solution

This solution is required to relate the local wing angle of attack to its bound vorticity distribution, which must be such that the downwash it causes when added to the trailing system flow produces the downwash necessary to match the physical kinematic boundary conditions on the wing.

Consistent with lifting-line theory, it is assumed that the local downwash may be computed by considering the downwash of a two-dimensional system as shown in Ref. 1. This solution must match the kinematic and dynamic boundary conditions appropriate to a jet-flapped airfoil.

There are two approximate approaches to the problem of defining the bound vorticity. The first is to assume that the vorticity is composed of two parts—one being that of a two-dimensional jet-flap airfoil at $\alpha_1 = \alpha - \alpha$ with a jet flap of strength C_j and angle θ (Fig. 2). This gives a downwash field w_1. To satisfy the wing boundary condition, a further vorticity is required, and this is assumed to be that of a plain airfoil at α_2 giving downwash w_2. Thus, the kinematic boundary condition on the wing is exactly satisfied, and the dynamic boundary condition on the wake approximately satisfied. The above is called the alpha effective model. An alternative approximation is to assume the vorticity is that of a two-dimensional jet-flap airfoil at the true effective angle $\alpha - \alpha_i$ but at a reduced jet strength. The new effective blowing coefficient C_{je} is obtained by maintaining the same momentum lift in the three-dimensional wing as in a two-dimensional jet-flap airfoil.

$$C_j(\theta + \alpha - \alpha_\infty) = C_{j_e}(\theta + \alpha - \alpha_i) \tag{4}$$

This is called the C_j effective model.

Thus, the loss in jet effectiveness due to three-dimensional flow (involving the downwash due to the trailing vortex field) may be accounted for either by a reduced effective angle of attack or by a reduced effective momentum coefficient.

Combination of Trefftz and Wing Equations

It has been shown that introducing σ as an unknown requires two Trefftz and wing equations to close the set. The Trefftz plane solution gives unambiguous results for C_n and C_t. The wing plane gives two alternative expressions for C_n and C_t. In principle, four consistent sets could be chosen. For our purposes, the α effective assumption was selected for both C_n and C_t since this is slightly simpler algebraically.

Coefficients Using α Effective Assumption

The lift coefficient due to the jet-flap airfoil at α_1, θ is $C_{l\alpha}\alpha_1 + C_{l\theta}\theta$ (where $C_{l\alpha}$ and $C_{l\theta}$ are the lift slopes for the jet-flap airfoil at the appropriate C_j). Expressions for $C_{l\alpha}$ and $C_{l\theta}$ are given in Ref. 2. In addition, there is the lift due to the plain wing vorticity of a flat plate at α_2, $2\pi\alpha_2$. Thus, the lift coefficient is

$$C_l = 2\pi\alpha_2 + C_{l_\alpha}\alpha_1 + C_{l_\theta}\theta \tag{5}$$

Subtracting the jet momentum $C_j(\alpha_1 + \theta)$ in order to obtain the normal pressure lift coefficient gives

$$C_{l_p} = 2\pi\alpha_2 + (C_{l_\alpha} - C_j)\alpha_1 + (C_{l_\theta} - C_j)\theta \tag{6}$$

For the nose thrust, the singular behavior near the leading edge is required. This may be represented in the form of a nose source N_o as described in Ref. 3 such that the perturbation near the nose behaves like $N_o/X_o^{1/2}$ where X_o is the distance from the leading edge. This can be written for a two-dimensional jet flap as

$$N_o = N_{o_\alpha}\alpha + N_{o_\theta}\theta \tag{7}$$

where expressions for $N_{o\alpha}$, $N_{o\theta}$ are given in Ref. 3.

For the plain airfoil vorticity, $N_{o()\alpha} = 1.0$. Thus, the total nose sngularity constant is given by

$$N_o = N_{o_\alpha}\alpha_1 + \alpha_2 + N_{o_\theta}\theta \tag{8}$$

Hence the nose thrust is given by

$$C_t = 2\pi(N_{o_\alpha}\alpha_1 + \alpha_2 + N_{o_\theta}\theta)^2 \tag{9}$$

These expressions may now be coupled with the results from the outer solutions.

Coupling

Combining the Trefftz and Wing solutions, Eqs. (2) and (6), for the pressure lift coefficient gives

$$4\bar{\alpha}\phi/c - C_j(\bar{\alpha}\phi_y + \alpha + \theta) = 2\pi\alpha_2 + (C_{l_\alpha} - C_j)\alpha_1 + (C_{l_\theta} - C_j)\theta \quad (10)$$

Substituting the geometrical results

$$\alpha_1 = \alpha - \alpha_\infty = \alpha + \bar{\alpha}\phi_y\,; \quad \alpha_i = \sigma\alpha_\infty \quad (11)$$

gives

$$4\bar{\alpha}\phi/c = 2\pi(\sigma - 1)\bar{\alpha}\phi_y + C_{l_\alpha}(\alpha + \bar{\alpha}\phi_y) + C_{l_\theta}\theta \quad (12)$$

This is an alternative formulation of usual integral equation of lifting-line theory. The connection is discussed in Ref. 9.

Applying the same procedure to the thrust equations [Eqs. (3) and (9)] gives

$$4\pi\{N_{o_\alpha}(\alpha + \bar{\alpha}\phi_y) + N_{o_\theta}\theta + \bar{\alpha}\phi_y(1 - \sigma)\}^2 = (4\bar{\alpha}\phi/c)(\alpha + \bar{\alpha}\phi_y) + C_j\{\theta^2 - (\alpha + \alpha\phi_y)^2\} \quad (13)$$

Solution Technique

General

The procedure employed is to assume a σ distribution and use collocation methods to solve Eq. (12). Then the results of this solution are substituted into Eq. (13), and a new result for σ is obtained.

Normalization of Lift Equation

Putting $Y = 2y/b$, $X = 2x/b$, $c^* = c/c_{av}$, $c_{av} = S_w/b$, $A = b/c_{av}$, and $\Phi = \bar{\alpha}\phi c_{av}$ where b is the wing span, S_W the area, and c_{av} the mean chord and defining equivalent chord c_e and twist α_e gives

$$\alpha_e = (C_{l_\alpha}\alpha + C_{l_\theta}\theta)/4\pi\{C_{l_\alpha}/2\pi - (1 - \sigma)\} \quad (14)$$

$$C_e = 2c^*\{C_{l_\alpha}/2\pi - (1 - \sigma)\} \quad (15)$$

reducing Eq. (12) to

$$2\Phi/\pi c_e = \alpha_e + \Phi_y/A \quad (16)$$

It will be noted that Eq. (16) represents the *unblown* integrodifferential equation for an equivalent stretched twisted wing. If we knew $\sigma(y)$ we could determine c_e and α_e and then use standard unblown wing theory to solve for the potential. This could be a useful approximate technique for converting jet-flap wings into equivalent unblown wings so that standard available wing inversion programs can be used.

Potential Functions

Continuous potential

Writing the spanwise coordinate $\chi = \cos\omega$, the continuous potential Φc can be defined as

$$\Phi^c = \sum_{n=1}^{r-1} A_n \sin n\omega \quad (17)$$

$$\Phi_y^c = \frac{1}{\sin\omega}\sum_{n=1}^{r-1} nA_n \sin n\omega \quad (18)$$

It can be shown[10] that for r even if $\Phi_m{}^c$ is defined at the pivotal points $\omega = m\pi/r$ that Eq. (16) can be satisfied at the pivotal points yielding the linear equation

$$\sum_{n=1}^{r-1}\left(\frac{2}{A}\beta_{kn} + \frac{4}{\pi c_e(k)}\delta_{kn}\right)\Phi_n{}^c = 2\alpha_e(k) \quad (19)$$

where

$$\delta_{kn} = 1,\ k = n \qquad \delta_{kn} = 0,\ k \neq n \quad (20)$$

where β_{kn} is defined in Ref. 10.

Discontinuous potential

For discontinuous wing geometry, it is necessary to have a potential function which is continuous, with the proper behavior at the wingtips and at infinity and which has a finite jump in its derivative $\Phi_{i(y)}$ at a given station $\omega_{d(i)}$. As shown in Ref. 10, the function $\Phi_i{}^*$ which satisfies this can be written

$$\Phi_i{}^*(\omega) = \left[(\cos\omega - \cos\omega_{d_i})\ln\left\{\frac{\sin\left(\frac{\omega + \omega_{d_i}}{2}\right)}{\sin\left(\frac{\omega - \omega_{d_i}}{2}\right)}\right\} + \omega_{d_i}\sin\omega\right] \quad (21)$$

$$\Phi_{i_y}{}^*(\omega) = -H(\omega_{d_i} - \omega) \quad (22)$$

where H is the Heaviside function with the property

$$H(\omega_{d_i} - \omega) = 1 \text{ for } \omega \leq \omega_d \quad (23)$$

$$H(\omega_{d_i} - \omega) = 0 \text{ for } \omega > \omega_d \quad (24)$$

It can be seen in the analysis that this function is capable of exactly matching a discontinuity in either c_e or α_e at ω_d.

General discontinuous solution

It can be assumed that discontinuities in effective geometric data (c_e and α_e) occur at s points, given by $\omega_{d(i)}$, $i = 1 \ldots s$. Then the general potential can be written in the form

$$\Phi(\omega) = \sum_{n=1}^{r-1} A_n \sin n\omega + \sum_{i=1}^{s}\lambda_i\Phi_i{}^*(\omega) \quad (25)$$

where λ_i is the magnitude of the ith downwash discontinuity.

Substituting into Eq. (7) at pivotal points:

$$\sum_{n=1}^{r-1}\left(\frac{2}{A}\beta_{kn} + \frac{4}{\pi c_e}\delta_{kn}\right)\Phi_n{}^c + \sum_{i=1}^{s}\left\{\frac{2}{A}H\left(\omega_{d_i} - \frac{k\pi}{r}\right) + \frac{4}{\pi c_{e_k}}\Phi_i{}^*\left(\frac{k\pi}{r}\right)\right\}\lambda_i = 2\alpha_{e_k} \quad (26)$$

$$k = 1 \cdots r - 1$$

where at the kth pivotal point $c_{e(k)}$ is the equivalent chord $c_{e(k)}$ and α_{ek} is the equivalent chord $\alpha_{e(k)}$. This yields $r - 1$ linear equations for the $r - 1 + s$ unknowns, Φ_n and λ_i. The additional s equations are obtained by considering the jump condition at each discontinuity.

Jump Condition

The jump condition represents the fact that at discontinuities, various geometrical and potential parameters (for example, chord or potential gradient) undergo finite step changes in magnitude. For example, one might have inboard flap chord extension Δc at a spanwise station $x = \bar{x}$ so that for $x < \bar{x}$, $c = c_1 + \Delta c$ while for $x \geq \bar{x}$, $c = c_1$, while c was continuous elsewhere. For various mathematical operations it is very convenient to represent this for-

mally by a so-called jump operator which, although different in function, is somewhat like the operator $]_b^a$ used to define limits of a definite integral. This jump operator is written $|_d$ and defined by its operations on a general function $g(x)$ in the following way:

$$g(x)\,|_d = \operatorname*{Lim}_{\delta \to 0}\{g(d) - g(d+\delta)\} \tag{27}$$

For example, for the chordwise discontinuity described above $c(x)\,|_{\bar{x}} = \Delta c$, while for any other value $x \neq \bar{x}$, $c(x)\,|_x = 0$. Equation (26) can be written

$$\frac{4}{\pi}\Phi^c(\omega) + \frac{4}{\pi}\sum_{i=1}^{s}\lambda_i\Phi_i^*(\omega) = 2\alpha_e c_e - \frac{2}{A}c_e\sum_{i=1}^{s}\lambda_i H(\omega_{d_i} - \omega) - \frac{2}{A}c_e\sum_{n=1}^{r-1}\Phi_n^c\beta_n^*(\omega) \tag{28}$$

The jump operator is now applied at each discontinuity. Then, noting that Φ^c and Φ^* are continuous throughout, this gives

$$0 = 2\alpha_e c_e\,|_{\omega_{d_j}} - \frac{2}{A}c_e\,|_{\omega_{d_j}}\sum_{n=1}^{r-1}\Phi_n^c\beta_n^*(\omega_{d_j}) - \frac{2}{A}\{c_e\sum_{i=1}^{s}\lambda_i H(\omega_{d_i} - \omega_{d_j})\}\,|_{\omega_{d_j}} \qquad j = 1 \cdots s \tag{29}$$

Now, defining

$$\Delta(\alpha_e c_e)_j = (\alpha_e c_e)\,|_{\omega_{d_j}} \qquad j = 1 \cdots s \tag{30}$$

$$J_{ij} = \{c_e H(\omega_{d_i} - \omega_{d_j})\}\,|_{\omega_{d_i}} \qquad \begin{matrix} j = 1 \cdots s \\ i = 1 \cdots s \end{matrix} \tag{31}$$

$$\beta_n^{**}(\omega_{d_j}) = \{\beta_n^*(\omega_{d_j})c_e\}\,|_{\omega_{d_j}} \qquad \begin{matrix} j = 1 \cdots s \\ n = 1 \cdots r-1 \end{matrix} \tag{32}$$

the set obtained is

$$\sum_{n=1}^{r-1}\beta_n^{**}(\omega_{d_j})\Phi_n^c + \sum_{i=1}^{s}J_{i_j}\lambda_i = A\Delta(\alpha_e c_e)_j \qquad j = 1 \cdots s \tag{33}$$

This provides the remaining s linear equations. Equations (26) and (33) are then inverted for the solutions Φ_n^c and λ_i.

Numerics and Iteration Process

General

The procedure used is to solve Eqs. (26) and (33) for $\sigma = 0.5$, then to substitute the values of Φ into the auxiliary thrust equation to determine a new set of σ values and to iterate this until the maximum change in σ is less than an arbitrary assigned value.

The program was written with the capacity to handle 8 points of discontinuity and 21 pivotal points. The only numerical constants required are the blown lift coefficient slopes. Since there are slight variations in these as quoted by different authors, Ref. 1 was used here. Four iterations are required to bring the changes in σ down to 10^{-5} so that convergence in all cases is very rapid. Programed on the CDC 6600, a given wing planform takes less than 2 sec to run. The program is written with attention to divisors, so that case $C_j = 0$ can be treated directly. Thus, plain unblown discontinuous wing may also be handled by the program.

Local Integral Properties

Three items of interest are the local lift, induced angle at infinity, and induced drag. If Φ is the solution, it can readily be shown that

$$C_l = 4\phi/c^* - 2C_j\phi_Y/A \tag{34}$$

$$\alpha_\infty = -2\phi_Y/A \quad , \quad C_{d_i} = C_l\alpha_\infty/2 \tag{35}$$

These coefficients can be integrated across the span (taking due account of singularities) to give the integral wing properties C_L and C_{DI}.

Thickness Effect

The preceding analysis is done for airfoils of zero thickness. The thickness effect can approximately be incorporated by using a modified lift slope in the wing-plane equation, as is normally done in the lifting-line approach to wing theory.

On this basis, the lift slope of a plain wing of finite thickness can be written as $2\pi\eta$ and that of the jet-flap wing of thickness t as $C_{l\alpha}{}^t$ and $C_{l\theta}{}^t$. Expressions for the latter quantities are derived in Ref. 9. Substituting these modified lift slopes into the wing-plane lift equation, it is found that the equivalent chord and angle of attack become

$$c_e = 2c^*\{C_{l_\alpha}{}^t/2\pi - \eta(1-\sigma)\} \tag{36}$$

$$\alpha_e = (C_{l_\alpha}{}^t\alpha + C_{l_\theta}{}^t\theta)/4\pi\{C_{l_\alpha}{}^t/2\pi - \eta(1-\sigma)\} \tag{37}$$

With these new definitions, Eq. (16) is unchanged.

Effective Aspect Ratio

Aspect ratio plays a dominant role as the scaling parameter in the lifting-line equation since the solution depends on it in a continuous, but nonlinear, fashion. For blown wings, the significance of the geometrical aspect ratio is obscured by the additional parameters C_J and θ. However, it can be shown that, for an elliptically loaded blown wing, an equivalent aspect ratio can be defined which has many useful properties.

The basic integral equation for the jet-flap wing is

$$4\Phi/c^* = C_{l_\alpha}\alpha + C_{l_\theta}\theta + \{C_{l_\alpha} - 2\pi(1-\sigma)\}2\Phi_Y/A \tag{38}$$

Differentiation with respect to α gives

$$4\Phi_\alpha/c^* = C_{l_\alpha} + \{C_{l_\alpha} - 2\pi(1-\sigma)\}2\Phi_{\alpha_Y}/A \tag{39}$$

An unblown wing, where $\sigma = \frac{1}{2}$ and $C_{l(\alpha)} = 2\pi$, gives

$$2\Phi_\alpha/\pi c^* = 1 + \Phi_{\alpha_Y}/A \tag{40}$$

If

$$f = C_{l_\alpha}/2\pi \quad , \quad A_e/A = 1/2\{f - (1-\sigma)\} \tag{41}$$

Equation (39) becomes

$$2\Phi_\alpha/\pi f c^* = 1 + \Phi_{\alpha_Y}/fA_e \tag{42}$$

This converts Eqs. (39) and (40) into identical equations. If f and σ are not functions of spanwise position, Eq. (42) can be solved by using standard theory for an unblown wing of aspect ratio A_e.

For the elliptically loaded case, this assumption of spanwise invariance is valid and f can be determined from two-dimensional jet-flap theory. However, σ cannot be determined without an auxiliary equation. Assuming σ is known, where C_L is the mean wing lift coefficient, Eq. (42) can be solved to obtain

$$C_{L_\alpha}/C_{l_\alpha} = (1 + 2C_J/\pi A_e)/(1 + 2/A_e) \tag{43}$$

where $C_{l(\alpha)}$ is the two-dimensional lift slope. An identical result can be shown for $C_{L(\theta)}$. Thus, the interesting general result that can be obtained is

$$C_L/C_l = (1 + 2C_J/\pi A_e)/(1 + 2/A_e) \tag{44}$$

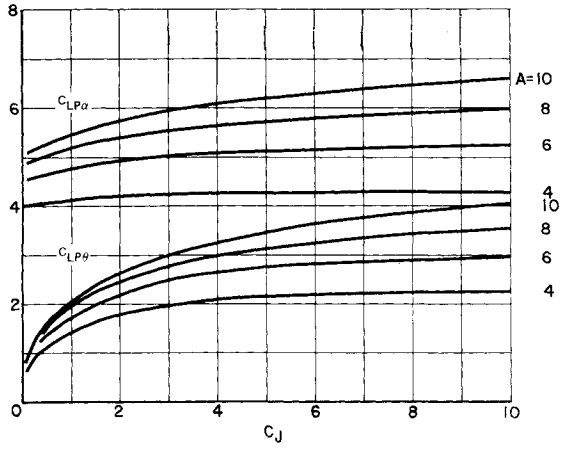

Fig. 3 Pressure lift gradients for rectangular wing of zero thickness.

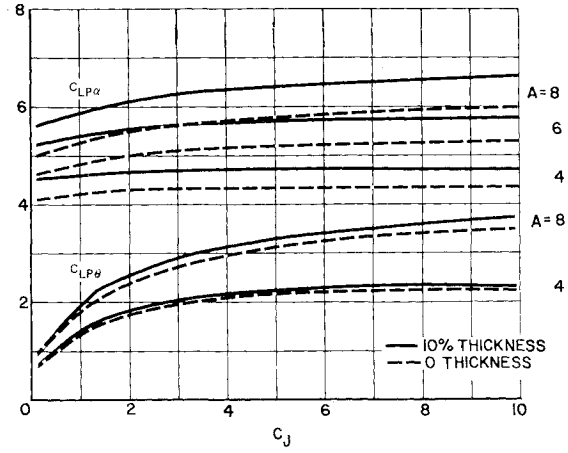

Fig. 4 Pressure lift gradients for rectangular wing of finite thickness.

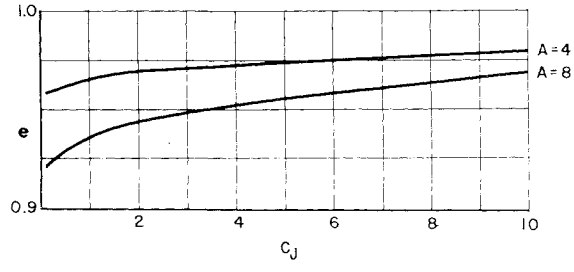

Fig. 5 Induced drag efficiency for rectangular wings.

This result is true for all elliptically loaded high-aspect-ratio wings—blown or unblown. The induced drag may also be written as

$$C_{D_I} = C_L^2/e(\pi A + 2C_J) \tag{45}$$

where e is an induced-drag efficiency which will be less than unity.

For a wing of arbitrary loading, f and σ will in general vary across the span; however, these equations will be approximately valid for some mean values f and $\bar{\sigma}$ where

$$A_e = A[2\{\bar{f} - (1 - \bar{\sigma})\}] \tag{46}$$

It should be noted in this representation σ must be known and cannot, in fact, be determined without solving the lift and thrust equations. However, these results can be useful if an estimate for σ is known from previous experience.

Results and Comparison with Theory and Experiment

Check of Analysis

The various known limit cases are correctly obtained with this model. Putting the aspect ratio equal to infinity recovers the proper two-dimensional jet-flap airfoil performance. For elliptical loading, a constant σ across the span is obtained with uniform downwash and lift coefficients. For zero blowing, the proper lifting-line solution for the wing is obtained. The discontinuous input was found to check with results given in Ref. 10 for an unblown wing with twist discontinuities. Other tests are described in Ref. 9.

Basic Results

There is such a large set of results available from the program that it is of no particular value to display wing performance for some arbitrary set of geometries. The elliptical cases have already been given in Ref. 1. Thus, for design purposes, the next most generally significant wing might be considered to be the constant-chord straight wing with constant spanwise blowing. A series of results for varying aspect-ratio and blowing coefficients are shown in Fig. 3 for rectangular wings of 0% thickness.

It is convenient here to plot only the pressure-lift coefficient; that is, the wing-system lift after the jet-momentum contribution has been subtracted. Typically, at a station, the pressure-lift coefficient is given by

$$C_{l_p} = C_l - C_j(\theta + \alpha)$$

while the wing-pressure-lift coefficient is given by

$$C_{L_p} = \frac{1}{S}\int C_{l_p} cdb$$

It should be noted that C_{Lp} is the significant term in any evaluation of the solution technique, since the momentum lift may be mechanically and exactly computed for any planform. By removing the momentum lift, differences in the solution approach may be more clearly identified. Because of the linearity of the analysis, the results are further condensed by considering only the gradients with α and θ—that is, $C_{Lp\alpha}$ and $C_{Lp\theta}$. It can be seen from Fig. 3 that this results in a fairly compact presentation of performance. It is also noteworthy, that for blowing coefficients above 4, there is little variation in the lift slopes with increasing C_j.

The thickness effect is very significant. An unblown wing of constant thickness can be accounted for by writing $2\pi\eta$ as the section lift slope; then, the lift slope of the thick wing becomes η multiplied by the lift slope of a 0% thick wing of aspect ratio A/η. The effect is to increase the three-dimensional lift slope by an amount somewhat less than η. A similar effect occurs for the blown wing; however, this is rather large when referred to pressure lift. Figure 4 shows pressure-lift slopes for 0% thick and 10% thick wings. Note that thickness is as significant as aspect ratio in determining performance. This point becomes important in comparing the theory with analytical results.

The generalized induced drag efficiency e (Fig. 5) is a useful quantity showing how well a given wing approaches its minimum blown induced drag. The efficiency values are quite high and suggest that for uniform blowing the induced drag of rectangular wings can be approximated by the well-known elliptical blown induced-drag expression.

Comparison with Other Theories

The analysis is an approximation of the actual lifting surface model, which is itself an idealization of the actual flow; thus the comparison of existing theoretical ap

Table 1 Ratio of wing lift to section lift for 0% thick aspect-ratio 6 wing

		$C_J = 1.0$	$C_J = 2.0$	$C_J = 0.0$ (Glauert[11])
Elliptical planform	Maskell & Spence ($\sigma = 0.5$)	0.699	0.680	
	Maskell & Spence (correct σ)	0.700	0.702	0.751
	Kerney	0.740	0.743	
Rectangular planform	Tokuda	0.726	0.700	
	Lopez & Shen	0.683	Not avail.	
	Lissaman ($\sigma = 0.5$)	0.664	0.656	0.720
	Lissaman (correct σ)	0.675	0.668	

Table 2 Effect of thickness on pressure-lift-curve slope

Planform	$C_{L_{(p\alpha)}}{}^t/C_{L_{(p\alpha)}}{}^o$ $C_J = 0$	$C_J = 2.0$
Elliptical	1.075	1.100
Rectangular	1.046	1.102

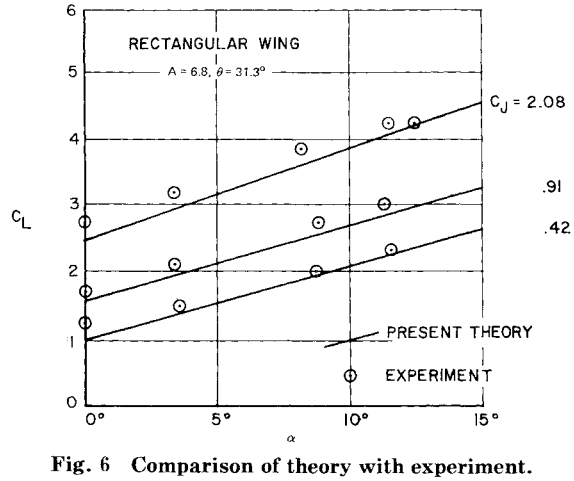

Fig. 6 Comparison of theory with experiment.

proaches should initially be discussed. The present paper is a lifting-line analysis and, in this respect, is similar to Maskell and Spence,[1] Kerney,[6] Tokuda,[7] and to the section design method of Lopez and Shen.[8] The latter three methods do not use an auxiliary equation to determine σ, but assume it has its unblown value of ½.

For elliptical loadings, the present model correlates with that of Maskell and Spence,[1] being a generalization of their technique, with a slightly different form of the auxiliary equation. The critical test of the lifting-line/auxiliary-equation model is the comparison with a properly numerically modeled linearized lifting-surface theory, with the appropriate kinematic and dynamic boundary conditions applied to a wing of zero thickness. The only existing lifting-surface model properly satisfying the wake boundary conditions is that of Lopez and Shen,[8] which shows excellent correlation with Maskell and Spence.[1] The present model can thus be considered verified for elliptical loading.

The rectangular wing presents a more difficult problem of correlation. Published solutions are given by Tokuda[7] and Lopez and Shen[8]; these solutions differ by small but significant amounts. To illustrate the differences between the various models, Table 1 shows the ratio of the wing lift to the section lift (C_L/C_l) for a representative design case—elliptical and rectangular wings of aspect ratio 6.0 at the blowing coefficients of 1.0 and 2.0. For this Table, the data from Ref. 8 was read from a graph; while for Tokuda's result,[7] his Eq. (6.6) was used. This equation is taken as

$$C_L/C_l = 1/[1 + \{\ln(8A/C_{l_\alpha}) + 1.577\}C_{l_\alpha}/4\pi A] \quad (47)$$

This form is written out since there is some ambiguity in the expression of Eq. (6.6) in Ref. 7. Classical lifting-line unblown ($C_J = 0$) results are shown in the last column. The present paper correlates rather well with the lifting-surface solution[8] while Tokuda's result[7] is somewhat higher. It can be concluded that the present analysis correlates with the lifting-surface approach, at least in this range.

In constructing Table 1, σ was used as defined in the present paper; however for the Spence and Maskell,[1] our σ was properly transformed according to definition of terms in Ref. 1.

Table 1 also shows that there is about as much variation in solutions between the rectangular and the elliptical planform as in the different analytical approaches. Although all solutions are probably acceptable for preliminary design purposes, it would be very valuable to have a few known exact solutions to test approximate methods against.

The effect of thickness of lift slope is very significant and appears to be larger for the blown wing than a plain wing. Some representative results are shown in Table 2 where the thickness correction of Ref. 1 is used for the blown elliptical wing, and the present method used for the rectangular wing. In Table 2, the ratio of $G_{Lp\alpha}{}^t$ for a 10% thick aspect-ratio 6 wing to $C_{Lp\alpha}{}^o$ is presented. It can be seen from Fig. 4 that a 10% thick aspect-ratio 6 wing has about the same performance as a 0% thick aspect-ratio 8 wing.

Comparison with Experiment

Comparison with experiment is a difficult process because few carefully controlled tests exist. Difficulties in proper normalization of experimental data involve not only the usual problems of viscous boundary-layer effects which occur with all wings, but the special jet-flap problems relating to proper determination of jet coefficient and jet angle, as well as the problem of proper wind-tunnel corrections for a jet-flap wing. Apparently, approximate thickness corrections and the use of an experimental effective aspect ratio can be used to fit a theoretical solution to almost any experimental data. As an illustration of this point, Fig. 6 shows a comparison of the present theory with the experimental results of Williams and Alexander.[12] The curves of the present theory were obtained by directly inserting the given data (planform, aspect ratio, thickness, angle of attack, blowing coefficient, and jet angle) into the program with no "corrections." The correlation is very good for lift slope, but there appears to be a systematic error in the lift at 0° angle of attack. This could be because the jet is not actually issuing at its nominal angle of 31.3°. It is of interest to note that after making an approximate global thickness correction, the results of Tokuda[7] match the experiment even more closely. However, Maskell and Spence[1] match the same data with a similar global thickness correction although their solution is for an elliptical wing with elliptical blowing, giving quite different results for C_L/C_l as shown in Table 1.

Conclusions

An analysis has been developed for high-aspect-ratio jet-flap wings of arbitrary geometry and blowing. It appears that the present method is as accurate as other known methods and is flexible and rapid, particularly for discontinuous planforms. Although definitive test data are lacking, correlation with existing experimental data is satisfactory. To properly evaluate jet-flap theories, it is recommended that definitive lifting-surface analyses be developed and properly controlled and corrected experiments conducted, including cases with discontinuous parameters. Finally, it is believed that the present method is a useful analytical tool for jet-flap wing design.

References

[1]Maskell, E. C., and Spence, D. A. "A Theory of the Jet Flap in Three Dimensions," *Proceedings of the Royal Society (London)*, Ser. A, Vol. 251, No. 1266, June 9, 1959, pp. 407–425.

[2]Spence, D. A., "The Lift Coefficient of a Thin, Jet-Flapped Wing," *Proceedings of the Royal Society (London)*, Ser. A, Vol. 238, No. 1212, Dec. 4, 1956, pp. 46–48.

[3]Lissaman, P. B. S., "A Linear Theory for the Jet Flap in Ground Effect," *AIAA Journal*, Vol. 6, No. 7, July 1968, pp. 1356–1362.

[4]Huckemann, D., "A Method of Calculating the Pressure Distribution over Jet Flapped Wings," R & M 3036, British Aeronautical Research Council, London, 1957.

[5]Hartunian, R. A., "The Finite Aspect Ratio Jet Flap," CAL Rept. A1-1190-A-3, Oct. 1959, Cornell Aeronautical Lab., Buffalo, N.Y.

[6]Kerney, K. P., "A Theory of the High Aspect Ratio Jet Flap," *AIAA Journal*, Vol. 9, No. 3, March 1971. pp. 431–435.

[7]Tokuda, N., "An Asympototic Theory of the Jet Flap in Three Dimensions," *Journal Fluid Mechanics*, Vol. 46, Pt. 4, April 27, 1971, pp. 705–726.

[8]Lopez, M. L. and Shen, C. C.," Recent Developments in Jet Flap Theory and Its Application to STOL Aerodynamic Analysis," AIAA Paper 71-578, 1971, Palo Alto, Calif.

[9]Lissaman, P. B. S., "Analysis of High-Aspect-Ratio Jet Flap Wings of Arbitrary Geometry," CR-2179, 1973, NASA.

[10]Multhopp, H., "The Calculation of the Lift Distribution of Aerofoils," R. T. P. Translation 2392, British Ministry of Aircraft Production, London.

[11]Glauert, H., *The Elements of Airfoil and Airscrew Theory*, Cambridge University Press, 2nd ed. 1948.

[12]Williams, J. and Alexander, A. J., "Three-Dimensional Wind-Tunnel Tests of a 30° Jet Flap Model," Conference Paper 304, British Aeronautical Research Council, London, 1957.

MAY 1974 J. AIRCRAFT VOL. 11, NO. 5

Aircraft Wake Vortex Transport Model

M. R. Brashears*
Lockheed Missiles & Space Company, Inc., Huntsville, Ala.
and
James N. Hallock†
DOT/Transportation Systems Center, Cambridge, Mass.

A wake vortex transport model has been developed which includes the effects of wind and wind shear, buoyancy, mutual and self-induction, ground plane interaction, viscous decay, finite core and Crow instability effects. Photographic and ground-wind vortex tracks obtained from DC-6, B-747, B-707, and CV-880 aircraft flybys are compared with predicted vortex tracks computed using meteorological and aircraft data as inputs to the transport model. A parametric analysis of the effects of the aircraft, fluid mechanic, and meteorological parameters shows the relative magnitude of each transport mechanism. The study constitutes the first detailed comparison of vortex transport theory with experimental data.

I. Introduction

AIRCRAFT wakes have long been recognized as safety and airport utilization problems. However, with the introduction of the large transport aircraft (B-747, DC-10, L-1011) and the ever increasing airport congestion, the wake vortex problem has taken on added significance. The vortices from large aircraft can present a severe hazard to other aircraft which inadvertently encounter the vortices; the following aircraft can be subjected to rolling moments which exceed the aircraft's roll control authority, to a dangerous loss of altitude, and to a possible structural failure. The probability of an aircraft-vortex encounter is greatest in the terminal area where light and heavy aircraft operate in close proximity and where recovery from an upset may not be possible due to the low aircraft altitude. To prevent aircraft-vortex encounters, the present solution (implemented by the Federal Aviation Administration in March 1970) has been to increase the separation standards behind the heavy jets. However, these increased separations decrease the capacity of the airport system and the present and predicted demands on airports cannot be met by just constructing additional runways and airports. Airport and airway system utilization are projected to double by 1980 and to increase five-fold by 1995. Technologically (using dual runways, improved landing aids, etc.), runway capacity can be substantially increased today, but not until the wake vortex problem and the inherent safety aspects have been alleviated.

There are two primary approaches to the wake vortex

Presented as Paper 73-679 at the AIAA 6th Fluid and Plasma Dynamics Conference, Palm Springs, Calif., July 16–18, 1973; submitted July 26, 1973; revision received January 23, 1974. The authors thank D. Burnham and T. Sullivan of TSC for providing the vortex tracking data prior to publication, K. Shrider of Lockheed-Huntsville for programing the model, and L. Garodz and N. Miller of NAFEC for providing their support during the testing and in the reduction of the rawinsonde and tower data.

Index category: Jets, Wakes, and Viscid-Inviscid Flow Interactions.

*Scientist Associate Research, Fluid Mechanic Applications Group. Member AIAA.

†Developmental Engineer, Wake Vortex Program. Member AIAA.